



جامعة الملك عبد الله
للعلوم والتقنية
King Abdullah University of
Science and Technology

A polydimethylsiloxane-coated metal structure for all-day radiative cooling

Item Type	Article
Authors	Zhou, Lyu; Song, Haomin; Liang, Jian Wei; Singer, Matthew; Zhou, Ming; Stegenburgs, Edgars; Zhang, Nan; Xu, Chen; Ng, Tien Khee; Yu, Zongfu; Ooi, Boon S.; Gan, Qiaoqiang
Citation	Zhou, L., Song, H., Liang, J., Singer, M., Zhou, M., Stegenburgs, E., ... Gan, Q. (2019). A polydimethylsiloxane-coated metal structure for all-day radiative cooling. Nature Sustainability, 2(8), 718–724. doi:10.1038/s41893-019-0348-5
Eprint version	Post-print
DOI	10.1038/s41893-019-0348-5
Publisher	Springer Nature
Journal	Nature Sustainability
Rights	Archived with thanks to Nature Sustainability
Download date	10/08/2022 05:09:25
Link to Item	http://hdl.handle.net/10754/656559

A polydimethylsiloxane coated metal structure for all-day radiative cooling

Lyu Zhou^{1,*}, Haomin Song^{1,2,*}, Jian-Wei Liang^{2,*}, Matthew Singer¹, Ming Zhou³, Edgars Stegenburgs², Nan Zhang¹, Chen Xu⁴, Tien Khee Ng², Zongfu Yu^{3,†}, Boon Ooi^{2,†}, Qiaoqiang Gan^{1,†}

1 Department of Electrical Engineering, The State University of New York at Buffalo, Buffalo, NY 14260, USA.

2 Photonics Laboratory, King Abdullah University of Science and Technology (KAUST), Thuwal 23955-6900, Saudi Arabia

3 Department of Electrical and Computer Engineering, University of Wisconsin, Madison, Wisconsin 53705, USA

4 School of Life Information Science and Instrument Engineering, Hangzhou Dianzi University, Hangzhou 310018, Zhejiang Province, China

* These authors contribute equally to this work.

† Email: zyu54@wisc.edu; boon.ooi@kaust.edu.sa; qqgan@buffalo.edu

Abstract- Radiative cooling is a passive cooling strategy with zero consumption of electricity, and it can be used to radiate heat from buildings to reduce air conditioning requirements. Although this technology can work well during optimal atmospheric conditions at nighttime, it is essential to achieve efficient cooling during daytime when peak cooling demand actually occurs. In this article, we report an inexpensive planar polydimethylsiloxane (PDMS)/metal thermal emitter, i.e., a thin film structure, which was fabricated using a fast solution coating process that is scalable for large area manufacturing. By performing tests under different environmental conditions, temperature reductions of 9.5 °C and 11.0 °C were demonstrated in the laboratory and out-door environment, respectively, with an average cooling power of ~120 W/m² for the thin film thermal emitter. In addition, a spectral-selective structure was designed and implemented to suppress the solar input and control the divergence of the thermal emission beam. This enhanced the directionality of the thermal emissions, so the emitter's cooling performance was less dependent on the surrounding environment. Out-door experiments were performed in Buffalo NY realizing continuous all-day cooling of 2~9 °C on a typical clear sunny day at Northern United States latitudes. This practical strategy that cools without electricity input could have a significant impact on global energy consumption.

(Length of the text: 3,226 words)

(Length of methods: 412 words)

(Length of legends: 450 words)

(Number of references: 41)

(Number and estimated final size of figures and tables: 5 figures)

Air conditioning is a significant end-use of energy and a major driver of global peak electricity demand. For instance, air conditioning consumes ~15% of the primary energy used by buildings in the United States^{1,2} and a shocking 70% of total electricity consumption in some tropical countries (e.g. Saudi Arabia³). Therefore, a passive cooling strategy that cools without any electricity input could have a significant impact on global energy consumption. The Earth's atmosphere has a transparent window for electromagnetic (EM) waves between 8-13 μm , which corresponds to the peak thermal radiation spectral range of terrestrial objects at typical ambient temperatures (e.g. ~20 °C to 45 °C). This transparent window is a cooling channel, through which an object on the Earth's surface can radiate heat into the cold of outer space. In studies of heat management in modern buildings, color and material properties of roofs and windows have been exploited for radiative cooling for decades (e.g. ref. [4], [5]). However, most conventional radiative cooling technologies only work at nighttime since solar heating is dominant during the daytime. To realize the envisioned all-day continuous cooling, it is essential to achieve efficient radiative cooling during the daytime, when peak cooling demand actually occurs⁶⁻⁹.

Recently, record-breaking daytime radiative cooling strategies have been demonstrated experimentally using various macro and micro structures designed for thermal radiation wavelengths. These structures are called thermal photonic structures and include planar multi-layered photonic films,¹⁰ hybrid metamaterial films¹¹ and polymer structural materials¹² with a reported cooling power of ~100W/m² during a sunny day with a clear sky. In addition, photonic structures with high visible-to-infrared (IR) radiation transparency and strong thermal emissivity have been reported, which is particularly useful for improved operation of solar panels^{13, 14}. These pioneering works demonstrated the potential to realize daytime radiative cooling with no electricity consumption¹⁵⁻²⁰. This technology can be used to assist climate control in buildings and significantly reduce energy usage²¹⁻²⁷. Therefore, enhanced radiative cooling technology represents a new research topic with a significant impact on the energy sustainability¹⁰⁻³⁸. In most literature published recently, people focused on optimizing or fabricating photonic (light-transmitting) structures with spectral-selective materials for daytime radiative cooling (e.g. [10-12]). One of the most attractive features associated with radiative cooling is the potential to reduce electricity consumption for cooling in metropolitan areas [21]. However, advanced thermal photonic structures suffer from high fabrication costs and problems with scalability. Therefore, reducing the manufacturing cost and enhancing the scalability of these structures remain key research objectives (e.g. ref. [11, 12, 27]). Furthermore, although most papers present out-door test results, actual implementation within the limitations of a complex urban environment of crowded buildings has never been explored.

In this article, we report an inexpensive planar polydimethylsiloxane (PDMS)/metal thermal emitter thin film structure that is useful for efficient radiative cooling applications over large areas. By manipulating the beaming effect of the thermal radiation, a temperature reduction of 9.5 °C was demonstrated in the laboratory environment using liquid nitrogen as the cold source. Thermal emissions from the planar thermal emitter are omnidirectional, so the radiative cooling performance is heavily dependent on the surrounding environment. In an urban environment, only the roofs of the highest buildings have full access to the sky. Thermal emissions from short buildings will be partially blocked by surrounding taller buildings, resulting in limited access to the open sky (see *Note. S1* and *Fig. S1* in the supporting material). Due to the enhanced directionality of the thermal emitter, its radiative cooling performance has minimal dependence on the surrounding environment. In addition, a spectral-selective solar shelter architecture was designed and implemented to suppress the solar input during the daytime. Out-door experiments were performed in Buffalo NY, and the PDMS/metal thermal emitter realized continuous all-day radiative cooling with an optimal temperature reduction of 11.0 °C and an average cooling power of ~120 W/m² on a typical clear sunny day at Northern United States latitudes.

Designing the planar PDMS coated metal thermal emitter

PDMS is a promising inexpensive material for daytime radiative cooling due to its transparency in visible regime and strong thermal emissivity in the mid-infrared regime.³⁹ Here we propose a simple planar

PDMS/metal (Al or Ag) film structure to realize an inexpensive thermal emitter for radiative cooling, as illustrated in **Fig. 1A**. For a 150- μm -thick PDMS film, the optical absorption in visible to near IR spectrum domain is relatively weak (see the inset of **Fig. 1B** for the measured data). According to Kirchhoff's law, the absorption of the emitter corresponds to its emissivity. Importantly, one can see from measured data shown in Fig. 1B (spheres) that its optical absorption/emissivity in the mid-infrared spectral range is strong, agreeing well with the numerical modeling (see the solid curve, the optical data of PDMS are shown in **Fig. S2**). To reveal the thickness-dependence of this type of planar PDMS/metal thermal emitter, the absorption spectra of the thin film system was modeled as the function of the PDMS thickness (**Fig. 1C**). One can see obvious interference phenomenon in the wavelength range of 15-25 μm . The absorption/emissivity in the wavelength range of 8-13 μm is close to unity when the PDMS thickness is beyond 100 μm . Therefore, this structure is tolerant of large roughness in a PDMS film with thickness over 100 μm , which is convenient for inexpensive manufacturing over huge scales. We then employed a fast coating facility (**Fig. 1D**) to fabricate the PDMS layer with controlled thickness (see **Supplementary video 1**). As shown by the inset in **Fig. 1F**, we fabricated five samples and realized relatively stable control in thickness. Importantly, the strong emissivity in the 8-13 μm spectral window ($\sim 94.6\%$ of ideal blackbody radiation, see the shaded region in Fig. 1B) and weak absorption of solar energy (i.e., less than 10%) will enable the high performance daytime radiative cooling. Importantly, this planar thermal emitter is suitable for fast solution-based roll-to-roll manufacturing over large areas. Compared with a recently published new solution-based thermal emitter material for day-time cooling [12], this PDMS/Al structure is easier to fabricate at a much lower price due to its commercial availability. The ease of manufacturing and low cost nature of materials allow this technology to overcome the major barrier for implementation.

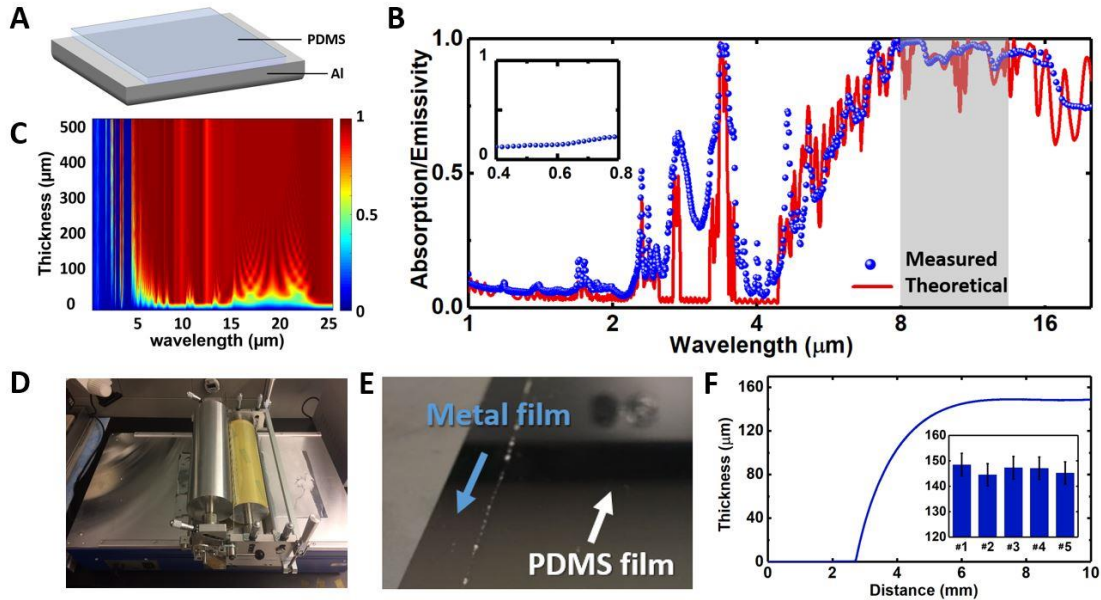


Figure 1| PDMS/metal thin film thermal emitter. (A) Schematic diagram of planar PDMS/metal thermal emitter. (B) Absorption/emissivity spectra of a planar PDMS/Al film with the thickness of 150 μm . Solid curve: numerical modeling; Spheres: measured data. (C) Modeled absorption spectra of the planar PDMS/Al film as the function of the PDMS film thickness. (D) A photograph of the PDMS coating facility under operation. (E) A photograph of the edge of a coated PDMS film on an Al plate. (F) A cross-sectional profile of a PDMS film. Inset: Measured thicknesses of five samples. The error bar arises from uncertainty in the measurements.

In-door experiment

The schematic diagram of the in-door experimental setup (see **Note S2** for detailed discussion) is shown in **Fig. 2A**: We filled a bottom thermal insulating foam tank with liquid nitrogen (at 77K). At the

bottom of this tank, we placed a black Al foil to function as the cold source by absorbing all thermal radiation (see **Fig. S3**). The PDMS/metal emitter was sealed by a polyethylene (PE) film in a thermal insulating foam container fixed at the top, facing down to the liquid nitrogen tank (**Fig. 2B**). Three temperature probes were placed at different positions, as indicated by D1-D3 in Fig. 2A. To reveal the divergence of the thermal emission from the PDMS/Al emitter, we characterized the angle dependent absorption at the wavelength of 10 μm . One can see in **Fig. 2C** that the measured thermal emission is approximately omnidirectional (left panel), agreeing very well with the numerical modeling result (right panel). Therefore, it is a technical challenge to collect the thermal radiation efficiently to optimize the radiative cooling performance. Beam control of the thermal emission (e.g. ref. [40]) is therefore of interest to address this limitation.

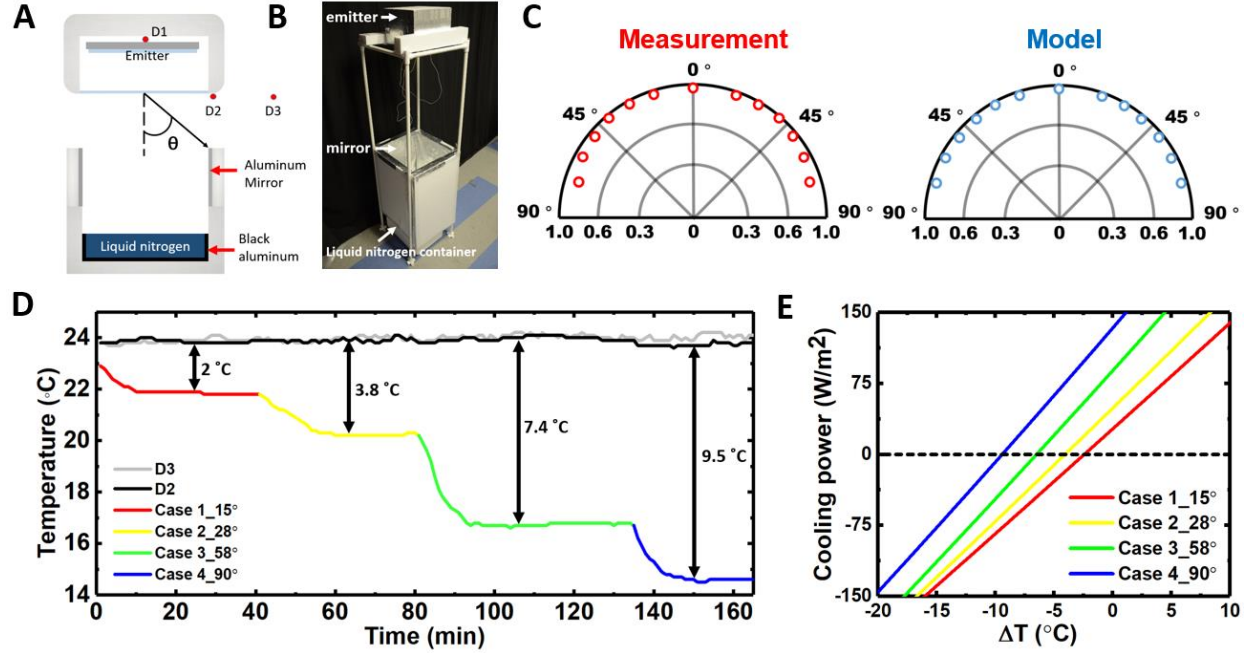


Figure 2. In-door radiative cooling characterization using liquid nitrogen as the cold source. (A) Schematic diagram of the experimental setup. (B) Photograph of the experimental setup. (C) Measured and modeled angle-dependent absorption distribution of the planar PDMS/Al cavity emitter at the wavelength of 10 μm . (D) Measured radiative cooling effect with different collection efficiencies (i.e., θ tuned from 15° to 90°). (E) Calculated cooling power of the 100- μm -thick PDMS/Al cavity emitter within different collection angles from 15° to 90°.

In this experiment, we partially or fully connected the output port of the emitter to the cold source using flat Al foils to form a rectangular waveguide tube for thermal emission. These Al mirrors were employed as the side wall to determine the collection angle, θ , as illustrated in Fig. 2A. As a result, cooling effects at different collection angles were observed experimentally, as shown in **Fig. 2D**. When θ was tuned from 15° to 90°, a temperature difference from 2 °C to 9.5 °C was obtained, depending on the collection efficiency of the thermal radiation. It should be noted that the measured temperature at D2 and D3 are almost the same (black and gray curves, respectively), indicating that the temperature around the emitter box was not affected by the convection of liquid nitrogen. Therefore, the observed cooling effect was mainly introduced by wave-guided thermal radiation.

To interpret the observed in-door radiative cooling performance, we then analyze the cooling power at each collection angle. The net cooling power, P_{net} , is defined below ¹⁰:

$$P_{net} = P_{rad}(T_{dev}) - P_{amb}(T_{amb}) - P_{cold\ source}(T_{LN2}) - P_{nonrad}(T_{dev}, T_{amb}) \quad (1).$$

Here, P_{rad} is the output power of the PDMS/Al emitter; P_{amb} and $P_{cold\ source}$ are incident radiation powers from the ambient and the cold source, respectively; $P_{nonrad}(T_{dev}, T_{amb})$ is the nonradiative power loss because of convection and conduction; T_{dev} is the temperature of the emitter; T_{LN2} is the temperature of liquid nitrogen, T_{amb} is the ambient temperature. Details of these parameters are listed in **Note S3**. Using this equation, the predicted cooling power of the system is plotted in **Fig. 2E** as the function of the temperature difference, ΔT (i.e., $T_{dev} - T_{amb}$). The intersection point at the cooling power of 0 W/m² indicates the achievable stabilized temperature difference. As the collection angle increases, the intersection points will shift to the left side, indicating the improved cooling performance. Here we calculated the cooling powers of the same emitter with four different collection angles of 15°, 28°, 58° and 90°, respectively, corresponding to the four experimental tests shown in Fig. 2D. The stabilized temperature differences at four intersection points of dashed line are -2.3 °C, -3.7°C, -6.5 °C and -9.2 °C, respectively, agreeing well with the measured results shown in Fig. 2D. Next, we continue to explore the radiative cooling performance by controlling the thermal emission angle in an out-door environment.

Out-door experiment

Radiative cooling was proposed to reduce the air-conditioning energy consumption. A clear sky is required for efficient thermal emission. However, how the surrounding environment near the emitter will affect the radiative cooling performance is a practical issue to justify the practical implementation of this passive cooling technology in urban areas. Before we perform the out-door experiment, it is necessary to analyze the angle dependence of the thermal emission first.

The emissivity/absorptivity of the atmosphere at the zenith angle, γ , can be described by ⁴¹

$$\varepsilon_{air}(\gamma, \lambda) = 1 - [1 - \varepsilon_{air}(0, \lambda)]^{1/\cos\gamma} \quad (2)$$

where $[1 - \varepsilon_{air}(0, \lambda)]$ is equal to the modeled atmospheric transmission spectrum shown as the blue curve in **Fig. 3A** (data from MODTRAN®). Using this equation, we plot the angle dependent atmospheric transmission at the wavelength of 10 μm in **Fig. 3B**, showing that the thermal emission to the real sky is no longer omnidirectional (in contrast to Fig. 2C). On the other hand, although the thermal emissivity reduces to ~75% at large emission angles, the structure still emits a significant part of its thermal energy at these angles. Therefore, if the thermal emission at these large angles is blocked in an outdoor environment by various surrounding architectures, the radiative cooling performance will be affected.

To reveal this environmental dependency, we performed outdoor tests at three different places at UB campus from 11:00 am to 3:00 pm on February 28th, 2018 (with a clear sky and the relative humidity of ~60 %). As shown in **Fig. 3C**, the planar PDMS/metal emitter was placed at the bottom of the high-density foam container sealed by the PE film. A foam board covered by highly reflective Al foils was placed next to the emitter container to serve as a shadow board (inspired by ref. [17], see also **Fig. S4**). It can create a shadow to block the direct sun light illumination (see the spectrum plotted by the yellow region in Fig. 3A), especially within the period with peak solar input. We employed a fish-eye lens to demonstrate the access to the clear sky (see upper panels in **Figs. 3D-3F**). One can see that the access to the clear sky is limited when the emitter is surrounded by tall buildings (Figs. 3D and 3E). Large open spaces like parking lots are ideal for radiative cooling (Fig. 3F). As a result, we obtained the temperature reduction of 2.5(± 0.3) °C in Fig. 3D, 7.2 (± 0.4) °C in Fig. 3E and 11 (± 0.2) °C in Fig. 3F, respectively. Using Eqs. (1, 2) (the temperature of the cold source is adapted to 3 K), we further modeled ΔT as the function of the collection angle (**Fig. 3G**). One can see that the estimated cooling performance (solid curve) agrees well with the experimental results extracted from Figs. 3D-3F (i.e., hollow dots). These results revealed a practical limitation to implement radiative cooling technology in urban areas: Although all buildings have the access to the clear sky on their roofs, the radiative cooling performance will be affected significantly by the surrounding architectures (See **Note S4** for the other discussion in outdoor radiative cooling test). To

overcome this practical limitation, we will propose an improved system design using beaming effect of thermal radiation.

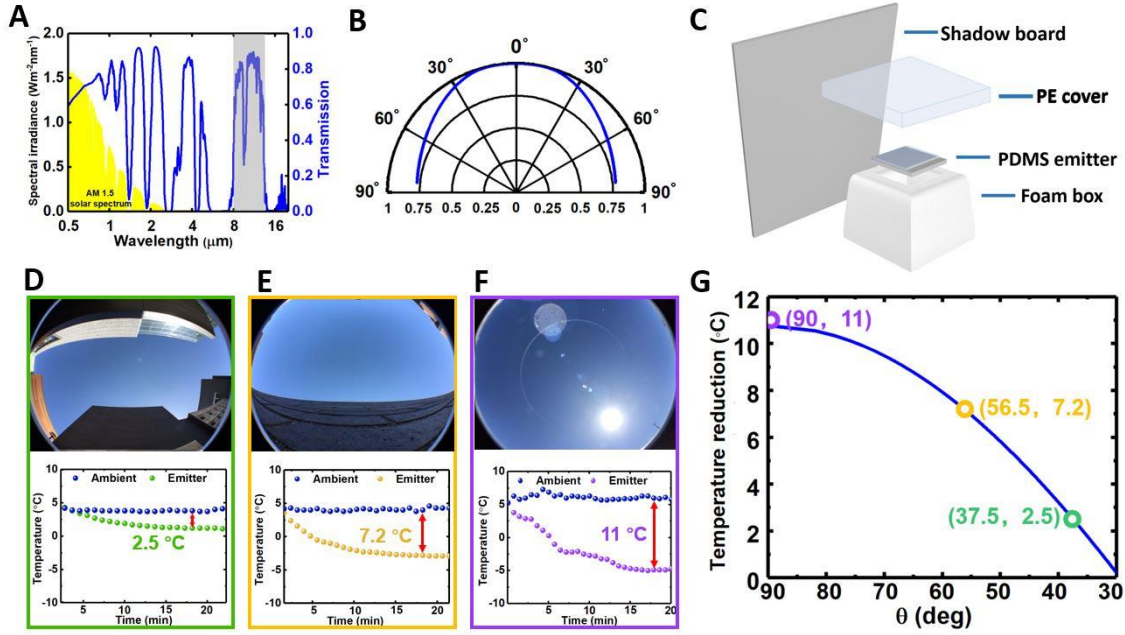


Figure 3. Out-door radiative cooling test over different emission angle. (A) Atmospheric transmission spectrum (blue curve) and the solar irradiation spectrum (yellow shaded region). (B) Modeled angle-dependent atmospheric transmission distribution at the wavelength of 10 μm. (C) Schematic of out-door radiative cooling test apparatus. (D)-(F) Measured temperature curves (lower panels) at different locations in UB (upper panels). (G) Calculated temperature reduction as the function of the collection angle (solid curve). Hollow dots: Measured data extracted from Figs. 3D~3F.

A spectral-selective beaming architecture

According to our calculation shown in Fig. 2E, the cooling power of the planar PDMS/Al system with a collection angle of 90° is ~120 W/m², corresponding to ~12% of the solar energy. However, as shown in the inset of Fig. 1B, the PDMS film still absorbs part of the solar irradiation in visible and near-infrared regime. In addition, the Al plates can also lead to the solar absorption at near-infrared wavelengths, which will considerably affect the cooling performance. Therefore, suppression of solar input is one of the most important technical issues for daytime cooling (e.g. ref. [10-22, 28, 29]). Although shadow board used in Fig.3C is a simple component, it is challenging to implement this architecture to completely block the sunlight in low-latitude tropic areas where cooling is most needed. In particular, if the incident angle is close to 90° at noontime in tropic areas, the shadow board will fail to block the sun light. Here we introduce a spectral-selective absorber material (Bluetec coating solar collector, see the inset in **Fig. 4A**) in the design of the radiative cooling system. Its optical absorption spectrum is shown as the blue curve in **Fig. 4A**, with near-unity absorption of solar illumination and very high reflection in the mid-IR domain (the ultimate target is to reproduce the ideal absorption spectrum as shown by the green curve). As illustrated in the left panel in **Fig. 4B**, we employed this spectral selective film to design a tapered waveguide to serve as a beaming component (See modeling in *Note S5* and **Fig. S5**). Therefore, most solar energy illuminated on its surface will be absorbed, while the thermal radiation from the planar thermal emitter can be reflected efficiently (right panel in **Fig. 4B**). Importantly, this material will not introduce much thermal emission back to the PDMS/Al emitter. At the center of the tapered waveguide, a smaller V-shaped shelter was introduced to block all normal incident solar light. As a result, the most important feature of this radiative

cooling enhancement component is its beaming effect on the mid-IR radiation and the suppression of the solar input. As shown by the numerical modeling results in **Fig. 4C**, the incident solar light was absorbed by the shelter film at a wide range of angle (including the normal incident angle), resulting in a negligible solar input during daytime. By optimizing the taper angle, the mid-infrared wave can be collimated and be confined within a relatively small spatial angle (lower panel in **Fig. 4D**) compared to the planar system (upper panel in **Fig. 4D**) (see more modeling details in *Methods*). Using this beam-controlled enhancement component (**Fig. 4E**), the impact of the surrounding environment in cooling performance can be greatly suppressed (e.g. see Fig. S1 in the supporting information). To validate this prediction, we still placed the system at those three locations at UB (Fig. 3D-3F) and characterized their radiative cooling performance (two temperature probes were placed at different positions, as indicated by the red dots in the right panel in Fig. 2B). One can see from **Fig. 4F-4H** that the temperature reduction is very similar, confirming the independence on the surrounding architectures. More intriguingly, this beam-controlled spectral selective architecture can enable all-day radiative cooling, as will be discussed next.

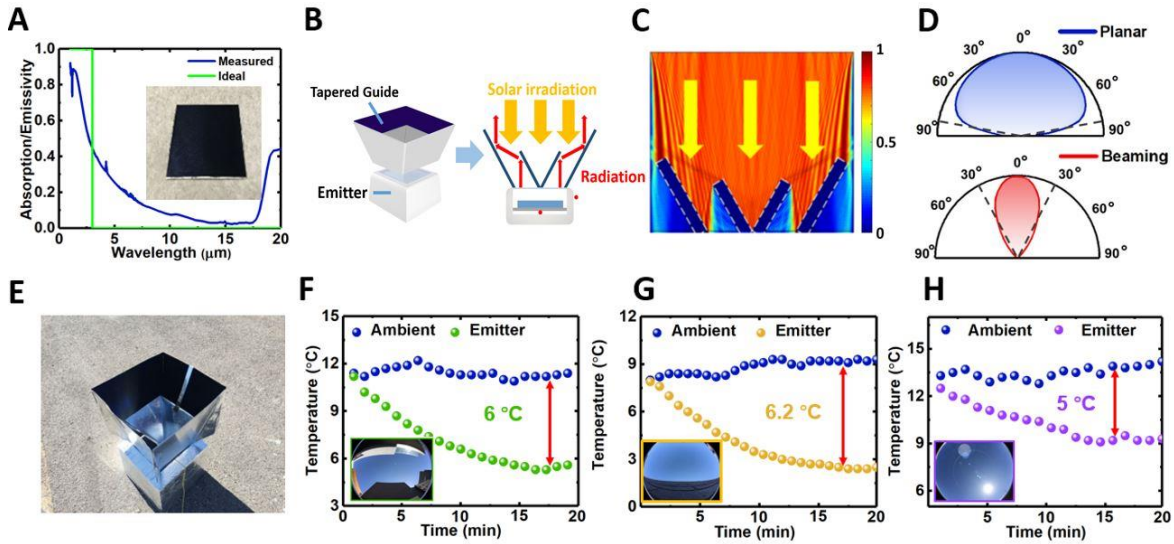


Figure 4. Beaming effect and solar shelter for daytime cooling. (A) Absorption spectra of an ideal selective absorber (the green line) and a commercial spectral selective absorber (the blue line), respectively. (B) Schematic diagram of the cooling system with tapered waveguide structure for thermal emission beam control and suppression of solar input. (C) Modeled beam propagation distribution with a normal incident solar light (at the wavelength of 500 nm) and (D) the output thermal beam propagation distributions for a planar system (upper panel) and a beaming system (lower panel) in mid-infrared wavelength region (at 10 μm). (E) The photograph of the beaming system. (F)-(H) Outdoor experimental results at the same three locations at UB in Figs. 3D-3F.

All-day continuous radiative cooling

Finally, we performed continuous experiment at a co-author's backyard at Buffalo from 6:00 pm on March 25 to 11:59 pm on March 27, 2018 (with a clear sky and the relative humidity of ~35%). The peak irradiation of sunlight was ~853.5 W/m². As shown in **Fig. 5A**, we placed a beaming system and a control system (with no beaming architecture, i.e., the system with a shadow board used in Fig. 3C) on the ground, ~5 meter away from the door of the house. As shown in **Fig. 5B**, three temperature curves were recorded for the ambient, the beaming system and the control system, respectively. Remarkably, the temperature in the beaming system was always lower than the ambient temperature. An obvious spike was observed on the first night due to a thin cloud on the direct top sky, reflecting the weather-dependency of radiative cooling (see *Note S6, Figs. S6, S7 and S8* for another out-door experiment performed at Thuwal, Saudi Arabia with a complete different weather condition). To further reveal the cooling performance, the

temperature differences in these two systems are plotted in **Fig. 5C**, showing that the beaming system reduced the temperature by 2~6 °C during the daytime and 7~9 °C at nighttime, respectively. Although the planer PDMS cooling system realized slightly better cooling performance at night (9~11 °C), its temperature is 4~6 °C higher than the surrounding in the morning since the sunlight was not always blocked by the shadow board. The V-shaped shelter structure realized all-day radiative cooling, which is highly desired in practical applications and simpler than a recently reported computer-controlled sensor feedback solar shelter system [20]. Under the peak of sun irradiance, the estimated cooling power is 76.3 W/m². Furthermore, to scale up this cooling architecture, one can implement modularized radiative cooling units with V-shaped shelter structures in an array rather than developing a huge area beaming architecture (see Fig. S9 in the supporting information for a schematic illustration). The actual performance and further optimization will depend on the local weather condition and the optical properties of spectral selective materials, which is under investigation but beyond the scope of this work.

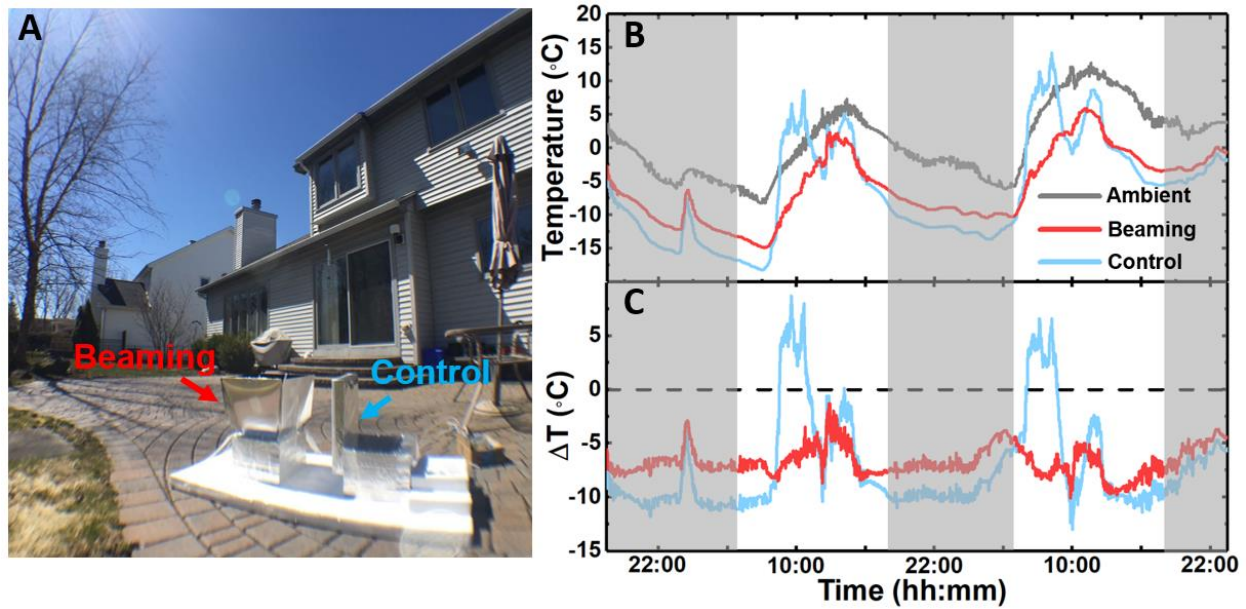


Figure 5. All-day continuous radiative cooling. (A) The photograph of the continuous radiative cooling experiment performed in the backyard of a house at Buffalo. (B) A continuous 50-hours cooling test: the grey line indicates the ambient temperature, the red line is the temperature in the beaming system, and the blue line is the temperature in the control system. (C) Temperature differences achieved in the beaming system (red curve) and the control system (blue curve), respectively.

Conclusions

In summary, we developed a highly efficient and low-cost passive cooling technology by exploiting the sky as the cold source. The proposed planar PDMS/Al cooling structures efficiently send invisible, heat-bearing light within the transparent window of the Earth's atmosphere (i.e., 8-13 μm) directly into the cold outer space and realized up to 11 °C temperature reduction. Using a spectral selective shelter component to suppress the solar input during the daytime, this technology realized a temperature reduction of 2~9 °C. Importantly, such passive cooling neither consumes energy nor produces greenhouse gases. Furthermore, due to the controlled thermal emission enabled by the tapered thermal light waveguide, the beaming radiative cooling system is insensitive to the surrounding building architectures, which is therefore suitable for the implementation in urban environment. All-day continuous cooling was experimentally demonstrated on a typical sunny day at Buffalo. The large-scale production cost of the surface structure is expected to be highly competitive compared to traditional active cooling methods (e.g. electric air conditioning) because of almost zero operation cost. The proposed technology thus has

disruptive potentials in transforming cooling solutions in a wide range of industrial and residential applications.

Methods

Preparation of PDMS planar emitter and characterization. The precursors of PDMS include polysiloxanes (Silicone Elastomer Base from Dow Corning) and silicone resin solution (Silicone Elastomer Curing Agent from Dow Corning). Polysiloxanes was mixed with the silicone resin solution at the ratio of 10:1 (i.e., polysiloxanes: silicone resin solution = 10 : 1) in a beaker. The PDMS coating was operated using the blade coating method on a multicoater (RK K303 Multicoater). The thickness of the PDMS film was controlled by the micrometer adjuster of the coating blade. The fast coating process is shown in **Supplementary video 1**. After that, the coated substrate was then heated under 60 °C for 2 hours in an oven. The film thickness was characterized using a probe profilometer (Veeco, Dektak 8 advance development profiler).

Absorption spectrum measurement. The reflection (R) and transmission (T) spectra of samples were measured using a UV-VIS spectrometer (Cary 7000 Universal Measurement Spectrophotometer, Agilent, in visible to IR range) and a Fourier-transformed-Infrared Spectrometer (Vertex 70, Bruker, in mid-IR range) with an angle module (Bruker A513 variable angle reflection accessory). The absorption spectra were then calculated using 1-R-T.

Cooling performance measurement. The temperature was measured using K-type thermocouples connected to a 4-channel K thermometer SD logger (resolution ± 0.1 °C, AZ instrument). The humidity was measured by a humidity data logger external sensors (Elitech GSP-6, accuracy $\pm 3\%$ RH (25 °C, 20%-90% RH) and $\pm 5\%$ RH (other)). The solar irradiation was measured using a standard photodiode power sensor (S121C, Thorlabs) with a compact power meter console (PM100 A, Thorlabs).

Beam tracing modeling for the thermal emission. The ray tracing modeling of the emitted thermal beam shown in Fig. 4D was performed using LightTools (©2018 Synopsys, Inc.). The 3D model of the beaming structure was developed in Pro/ENGINEER Creo Suite (© PTC) and imported into the LightTools. To simulate the emitted beam of the PDMS film, we introduced a surface with a hemisphere emission pattern as the light source. Two different cases (with and without the taper) were modeled in Fig. 4D to compare the difference introduced by the beaming structure. Dashed lines in Fig. 4D indicate the spatial angles where the emission intensity decreases to a half of the maximum value. One can see that the thermal emission from the planar system was approximately omnidirectional (i.e., the upper panel). With the beaming structure, the thermal emission was then confined within a relatively small spatial angle (i.e., the lower panel in Fig. 4D of the main text).

Data availability. The data that support the findings of this study are available from the corresponding author upon request.

References

1. J. K. Kelso, 2011 Building energy data book. *Department of Energy* (2012).
2. S. Chu, A. Majumdar, Opportunities and challenges for a sustainable energy future. *Nature* **488**, 294 (2012).
3. C. Segar, Renewable Augment Gas – Saudi Energy Mix. *The Journal of the International Energy Agency* **7**, 40-41 (2014).

4. M. Mahdavinejad, K. Javanrudi, Assessment of Ancient Fridges: A Sustainable Method to Storage Ice in Hot-Arid Climates. *Asian Culture and History* **4**, 133-139 (2012).
5. S. Catalanotti *et al.*, The radiative cooling of selective surfaces. *Solar Energy* **17**, 83-89 (1975).
6. S. Fan, Thermal Photonics and Energy Applications. *Joule* **1**, 264-273 (2017).
7. M. Hossain Md, M. Gu, Radiative Cooling: Principles, Progress, and Potentials. *Advanced Science* **3**, 1500360 (2016).
8. X. Sun, Y. Sun, Z. Zhou, A. Alam Muhammad, P. Bermel, Radiative sky cooling: fundamental physics, materials, structures, and applications. *Nanophotonics* **6**, 997-1015 (2017).
9. S. Buddhiraju, P. Santhanam, S. Fan, Thermodynamic limits of energy harvesting from outgoing thermal radiation. *Proceedings of the National Academy of Sciences* **115**, E3609 (2018).
10. A. P. Raman, M. A. Anoma, L. Zhu, E. Rephaeli, S. Fan, Passive radiative cooling below ambient air temperature under direct sunlight. *Nature* **515**, 540 (2014).
11. Y. Zhai *et al.*, Scalable-manufactured randomized glass-polymer hybrid metamaterial for daytime radiative cooling. *Science* **355**, 1062 (2017).
12. J.Mandal *et al.*, Hierachically porous polymer coatings for highly efficient passive daytime radiative cooling. *Science* **362**, 315 (2018).
13. L. Zhu, A. Raman, K. X. Wang, M. A. Anoma, S. Fan, Radiative cooling of solar cells. *Optica* **1**, 32-38 (2014).
14. W. Li, Y. Shi, K. Chen, L. Zhu, S. Fan, A Comprehensive Photonic Approach for Solar Cell Cooling. *ACS Photonics* **4**, 774-782 (2017).
15. L. Zhu, A. P. Raman, S. Fan, Radiative cooling of solar absorbers using a visibly transparent photonic crystal thermal blackbody. *Proceedings of the National Academy of Sciences* **112**, 12282 (2015).
16. Y. Shi, W. Li, A. Raman, S. Fan, Optimization of Multilayer Optical Films with a Memetic Algorithm and Mixed Integer Programming. *ACS Photonics* **5**, 684-691 (2018).
17. E. Rephaeli, A. Raman, S. Fan, Ultrabroadband Photonic Structures To Achieve High-Performance Daytime Radiative Cooling. *Nano Letters* **13**, 1457-1461 (2013).
18. H. Yuan *et al.*, Effective, angle-independent radiative cooler based on one-dimensional photonic crystal. *Opt. Express* **26**, 27885-27893 (2018).
19. Z. Chen, L. Zhu, A. Raman, S. Fan, Radiative cooling to deep sub-freezing temperatures through a 24-h day–night cycle. *Nature Communications* **7**, 13729 (2016).
20. B. Bhatia *et al.*, Passive directional sub-ambient daytime radiative cooling. *Nature Communications* **9**, 5001 (2018).
21. E. A. Goldstein, A. P. Raman, S. Fan, Sub-ambient non-evaporative fluid cooling with the sky. *Nature Energy* **2**, 17143 (2017).
22. R. Gentle Angus, B. Smith Geoff, A Subambient Open Roof Surface under the Mid - Summer Sun. *Advanced Science* **2**, 1500119 (2015).
23. X. Lu, P. Xu, H. Wang, T. Yang, J. Hou, Cooling potential and applications prospects of passive radiative cooling in buildings: The current state-of-the-art. *Renewable and Sustainable Energy Reviews* **65**, 1079-1097 (2016).
24. G. J. Lee, Y. J. Kim, H. M. Kim, Y. J. Yoo, Y. M. Song, Colored, Daytime Radiative Coolers with Thin-Film Resonators for Aesthetic Purposes. *Advanced Optical Materials* **6**, 1800707 (2018).
25. T. Hoyt, E. Arens, H. Zhang, Extending air temperature setpoints: Simulated energy savings and design considerations for new and retrofit buildings. *Building and Environment* **88**, 89-96 (2015).
26. W. Li, Y. Shi, Z. Chen, S. Fan, Photonic thermal management of coloured objects. *Nature Communications* **9**, 4240 (2018).
27. T. Li *et al.*, A radiative cooling structural material. *Science* **364**, 760 (2019).
28. P.-C. Hsu *et al.*, Radiative human body cooling by nanoporous polyethylene textile. *Science* **353**, 1019 (2016).

29. P.-C. Hsu *et al.*, A dual-mode textile for human body radiative heating and cooling. *Science Advances* **3**, No. e1700895 (2017).
30. J.-I. Kou, Z. Jurado, Z. Chen, S. Fan, A. J. Minnich, Daytime Radiative Cooling Using Near-Black Infrared Emitters. *ACS Photonics* **4**, 626-630 (2017).
31. S. Atiganyanun *et al.*, Effective Radiative Cooling by Paint-Format Microsphere-Based Photonic Random Media. *ACS Photonics* **5**, 1181-1187 (2018).
32. Y. Peng *et al.*, Nanoporous polyethylene microfibrils for large-scale radiative cooling fabric. *Nature Sustainability* **1**, 105-112 (2018).
33. T. M. J. Nilsson, G. A. Niklasson, Radiative cooling during the day: simulations and experiments on pigmented polyethylene cover foils. *Solar Energy Materials and Solar Cells* **37**, 93-118 (1995).
34. Z. Huang, X. Ruan, Nanoparticle embedded double-layer coating for daytime radiative cooling. *International Journal of Heat and Mass Transfer* **104**, 890-896 (2017).
35. K. D. Dobson, G. Hodes, Y. Mastai, Thin semiconductor films for radiative cooling applications. *Solar Energy Materials and Solar Cells* **80**, 283-296 (2003).
36. A. R. Gentle, A. Nuhoglu, M. D. Arnold, G. B. Smith, 3D printable optical structures for sub-ambient sky cooling. *SPIE Optical Engineering + Applications (SPIE, 2017)*, vol. 10369.
37. A. R. Gentle, G. B. Smith, Angular selectivity: impact on optimised coatings for night sky radiative cooling. *SPIE NanoScience + Engineering (SPIE, 2009)*, vol. 7404.
38. G. B. Smith, Amplified radiative cooling via optimised combinations of aperture geometry and spectral emittance profiles of surfaces and the atmosphere. *Solar Energy Materials and Solar Cells* **93**, 1696-1701 (2009).
39. A. Srinivasan, B. Czapla, J. Mayo, A. Narayanaswamy, Infrared dielectric function of polydimethylsiloxane and selective emission behavior. *Applied Physics Letters* **109**, 061905 (2016).
40. J.-J. Greffet *et al.*, Coherent emission of light by thermal sources. *Nature* **416**, 61 (2002).
41. C. G. Granqvist, A. Hjortsberg, Radiative cooling to low temperatures: General considerations and application to selectively emitting SiO films. *Journal of Applied Physics* **52**, 4205-4220 (1981).

Acknowledgements

This work was partially supported by the National Science Foundation (grand no. IIP-1745846, ECCS-1507312, CBET-1445934 and ECCS-1425648).

Author contributions

Q.G., B.O. and Z.Y conceived the idea and supervised the project. L.Z., H.S., J.L., E. S. and T. N. executed the experiments. All authors contributed to the analysis of the experimental results and modeling. L.Z., H.S., Z.Y., B.O. and Q.G. wrote the manuscript. All authors reviewed the manuscript. L.Z, H.S and J.L are co-first authors and contributed equally.

Competing interests

Q.G. and Z.Y. have founded a company, Sunny Clean Water LLC, seeking to commercialize the results reported in this paper.